Adaptive Harmonic Elimination in a Grid-Connected Three-Phase PV Inverter

G Chandra Sekhar [*], P Rama Krishna [**]

[*] Department of EEE, Amrita Sai Institute of Science & Technology, Paritala, Krishna Dt, A.P, India
[**] Department of EEE, Amrita Sai Institute of Science & Technology, Paritala, Krishna Dt, A.P, India

Abstract- In this paper, a simple three-phase grid-connected photovoltaic (PV) inverter topology consisting of a boost section, a low-voltage three-phase inverter with an inductive filter, and a step-up transformer interfacing the grid is considered. Ideally, this topology will not inject any lower order harmonics into the grid due to high-frequency pulse width modulation operation. However, the non-ideal factors in the system such as core saturation-induced distorted magnetizing current of the transformer and the dead time of the inverter, etc., contribute to a significant amount of lower order harmonics in the grid current. A novel design of inverter current control that mitigates lower order harmonics is presented in this paper. An adaptive harmonic compensation technique and its design are proposed for the lower order harmonic compensation. In addition, a proportional-resonant-integral (PRI) controller and its design are also proposed. This controller eliminates the dc component in the control system, which introduces even harmonics in the grid current in the topology considered. The dynamics of the system due to the interaction between the PRI controller and the adaptive compensation scheme is also analyzed. The proposed system is simulated in MATLAB/SIMULINK platform

Index Terms- DC-link voltage, Zero voltage switching, Renewable Energy (RE), Proportional Resonant Integral (PRI).

I. INTRODUCTION

Renewable sources of energy such as solar, wind, and geothermal have gained popularity due to the depletion of conventional energy sources. Hence, many distributed generation (DG) systems making use of the renewable energy sources are being designed and connected to a grid. In this project, one such DG system with solar energy as the source is considered.

The topology of the solar inverter system is simple. It consists of the following three power circuit stages:

1) a boost converter stage to perform maximum power point tracking (MPPT);
2) a low-voltage single-phase H-bridge inverter;
3) an inductive filter and a step-up transformer for interfacing with the grid.

Fig.1 shows the power circuit topology considered. This topology has been chosen due to the following advantages: The switches are all rated for low voltage which reduces the cost and lesser component count in the system improves the overall reliability. This topology will be a good choice for low-rated PV inverters of rating less than a kilowatt. The disadvantage would be the relatively larger size of the interface transformer compared to topologies with a high-frequency link transformer. The system shown in Fig. 1 will not have any lower order harmonics in the ideal case. However, the following factors result in lower order harmonics in the system: The distorted magnetizing current drawn by the transformer due to the nonlinearity in the B–H curve of the transformer core, the dead time introduced between switching of devices of the same leg [2]–[6], on-state voltage drops on the switches, and the distortion in the grid voltage itself. There can be a dc injection into the transformer primary due to a number of factors. These can be the varying power reference

from a fast MPPT block from which the ac current reference is generated, the offsets in the sensors, and A/D conversion block in the digital controller. This dc injection would result in even harmonics being drawn from the grid, again contributing to a lower power quality. It is important to attenuate these harmonics in order for the PV inverter to meet standards such as IEEE 519-1992 [7] and IEEE 1547-2003 [8]. Hence, this paper concentrates on the design of the inverter current control to achieve a good attenuation of the lower order harmonics. It must be noted that attenuating the lower order harmonics using a larger output filter inductance is not a good option as it increases losses in the system along with a larger fundamental voltage drop and with a higher cost. There has been considerable research work done in the area of harmonic elimination using specialized control. Multi resonant controller-based methods are used for selective harmonic elimination. The advantage of these methods is the simplicity in implementation of the resonant blocks. However, discretization and variations in grid frequency affect the performance of these controllers and making them frequency adaptive increases overall complexity. The phase margin of the system becomes small with multi resonant controllers and additional compensation is required for acceptable operation.
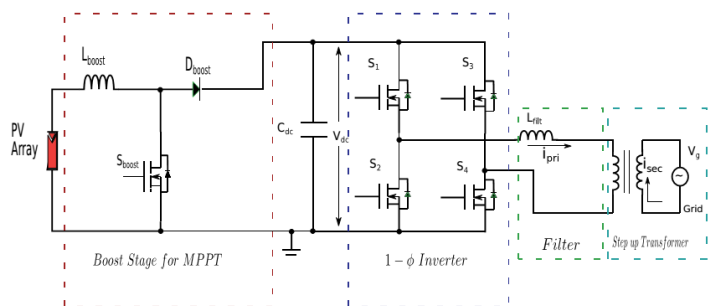
Fig. 1. Power circuit topology of the1−φPV system for a low-voltage inverter connected to grid using a step-up transformer.

In [16]–[19], adaptive filter-based controllers are considered for harmonic compensation. The study in [18] uses an adaptive filter to estimate a harmonic and then adds it to the main current reference. Then, a multi resonant block is used to ensure zero steady-state error for that particular harmonic reference. The advantage of the adaptive filter-based method is the inherent frequency adaptability which would result in same amount of harmonic compensation even when there are shifts in grid frequency. The implementation of adaptive filters is simple. Thus an adaptive filter-based method is proposed. This method estimates a particular harmonic in the grid current using a least-mean-square (LMS) adaptive filter and generates a harmonic voltage reference using a proportional controller. This voltage reference is added with appropriate polarity to the fundamental voltage reference to attenuate that particular harmonic.

This paper includes an analysis to design the value of the gain in the proportional controller to achieve an adequate level of harmonic compensation. The effect of this scheme on overall system dynamics is also analyzed. This method is simple for implementation and hence it can be implemented in a low-end digital controller. The presence of dc in the inverter terminal voltage results in a dc current flow into the transformer primary. This dc current results in drawing of even harmonics from the grid. If the main controller used is a PR controller, any dc offset in a control loop will propagate through the system and the inverter terminal voltage will have a nonzero average value. An integral block is used along with the PR controller to ensure that there is no dc in the output current of the inverter. This would automatically eliminate the even harmonics. This scheme is termed as proportional-resonant-integral (PRI) control and the design of the PRI controller parameters is provided.

II. OPERATION OF CONVERTER

In any inverter, the devices on the same leg are switched in a complementary fashion. In real devices, however, there is a finite switching time. Thus if complementary gate pulses were to be given to these switches directly, then there would exist a finite time when both the switches would not have turned off completely. This would result in shorting of the dc bus which is undesired. Hence a dead-time is introduced between the switchings of the devices of the same leg. Dead-time is the time during which the device which was ON would turn off. So, after the dead-time the device which was OFF could be turned ON.

For an inverter leg with switches S1 and S2, the pulses to be given ideally and the pulses with dead-time are shown in Fig.3.2. The dead-time t_d has to be at least equal to the turn-off time of the devices.

Now, to analyze the effect due to dead-time, consider Fig.4. In case-1, the top device is ON. The current at the pole is assumed to be in the direction shown. When the top device gets the turn-off command, the bottom would still be kept OFF to ensure the dc bus does not get shorted. During the dead-time when both the devices are OFF, the current would flow through the body diode of the bottom device.
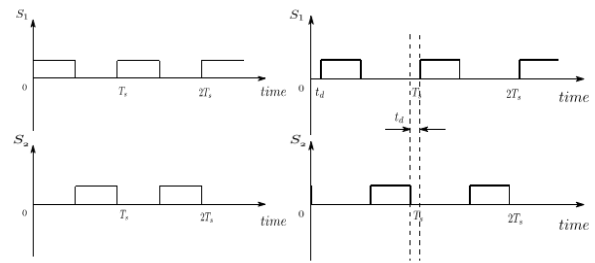
Fig 2. Switching logic pulses for a leg

This means that during the dead-time, when the current is positive, the pole voltage would be same as the case when bottom device is ON. Clearly from the Fig. 4, it can be observed that the average pole voltage falls by a fixed amount during positive half cycle of the current. Similarly, when the current is negative, it can be proved that the average pole voltage increases by the same amount. Thus, the dead-time effect on average pole voltage can be summarized in the following set of equations.

$$\Delta \overline{V}_{pole} = -\frac{V_{dc}t_d}{T_s} \qquad for \quad i > 0$$

$$\Delta \overline{V}_{pole} = \frac{V_{dc}t_d}{T_s} \qquad for \quad i < 0$$
$$\text{...............1}$$

Fig.3 shows the inductor current and the average pole voltage due to dead-time. This is for one leg of an inverter.
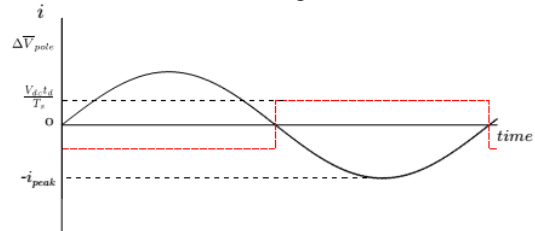
Fig 3. Error voltage due to dead-time
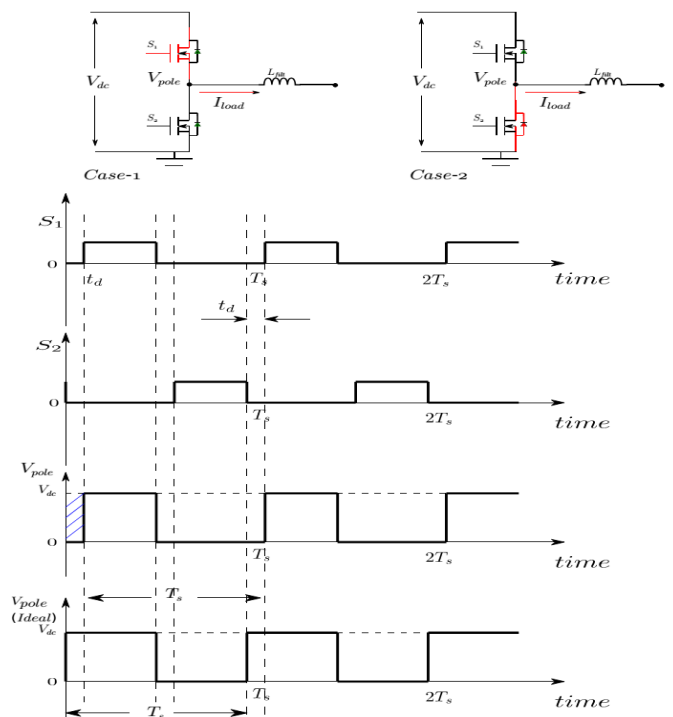
Fig 4. Dead-time influence on average pole voltage

The same analysis can be extended to the other leg of a H-bridge inverter. Fig.5 shows the schematic of a grid connected H-bridge inverter.
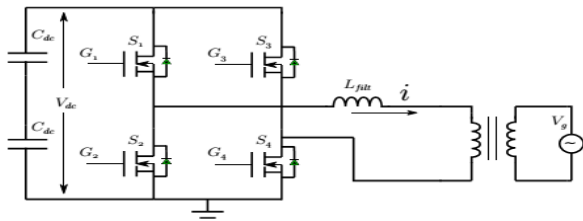
Fig 5. Schematic of a grid connected 1-φ inverter

For the leg containing switches S3 and S4, the error voltage due to dead-time would be same as in Fig. 3 except that there would be a phase lag of 180°. Thus the net voltage error that gets applied to the filter would be as shown in Fig. 6.
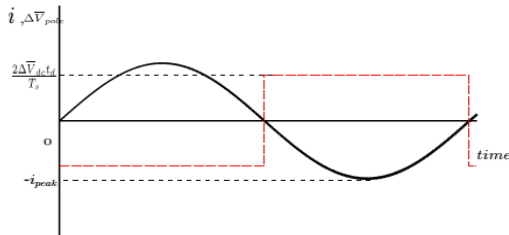
Fig 6. Net error voltage across filter

From the square wave nature of the voltage that is being applied, it can be clearly predicted that lower order harmonics would get injected into the grid. Hence the harmonic voltage peak due to the dead-time error voltage is given by:

$$V_n = \frac{2V_{dc}t_d}{nT_s} \qquad For \ odd \ n.$$

.......2

The phase of each odd harmonic would be 180^0 out of phase with respect to the inductor current. This Vn is responsible for injecting the lower order harmonic currents into the grid. It could be reduced by using an adaptive filter.

A) Odd Harmonics: The dominant causes for the lower order odd harmonics are the distorted magnetizing current drawn by the transformer, the inverter dead time, and the semiconductor device voltage drops. Other factors are the distortion in the grid voltage itself and the voltage ripple in the dc bus. The magnetizing current drawn by the transformer contains lower order harmonics due to the nonlinear characteristics of the B–H curve of the core. The exact amplitude of the harmonics drawn can be obtained theoretically if the B–H curve of the transformer is known.
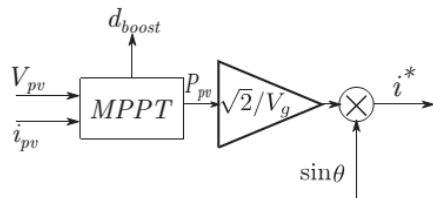
Fig. 7. Generation of an inverter ac current reference from an MPPT block.

The phase angle of the harmonics due to the magnetizing current will depend on the power factor of operation of the system. As the operation will be at unity power factor (UPF), the current injected to the grid will be in phase with the grid voltage.

However, the magnetizing current lags the grid voltage by 90◦. Hence, the harmonic currents will have a phase displacement of either +90◦ or −90◦ depending on harmonic order. The dead-time effect introduces lower order harmonics which are proportional to the dead time, switching frequency, and the dc bus voltage. The dead-time effect for each leg of the inverter can be modeled as a square wave error voltage out of phase with the current at the pole of the leg [2]–[6]. The device drops also will cause a similar effect but the resulting amount of distortion is smaller compared to that due to the dead time. Thus, for a single-phase inverter topology considered, net error voltage is the voltage between the poles and is out of phase with the primary current of the transformer. The harmonic voltage amplitude for a hth harmonic can be expressed as

$$V_{error} = \frac{4}{h\pi}\frac{2V_{dc}t_d}{T_s}$$

.......3

Where td is the dead time, Ts is the device switching frequency, and Vdc is the dc bus voltage. Using the values of the filter inductance, transformer leakage inductance, and the net series resistance, the harmonic current magnitudes can be evaluated. Again, it must be noted that the phase angle of the harmonic currents in this case will be 180◦ for UPF operation. Thus, it can be observed that the net harmonic content will have some phase angle with respect to the fundamental current depending on the relative magnitudes of the distortions due to the magnetizing current and the dead time.

B) Even Harmonics: The topology under consideration is very sensitive to the presence of dc offset in the inverter terminal voltage. The dc offset can enter from a number of factors such as varying power reference given by a fast MPPT block, the offsets in the A/D converter, and the sensors. To understand how a fast MPPT introduces a dc offset, consider Figs. 2 and 3. In Fig..2, dboost is the duty ratio command given to the boost converter switch, Vpv and ipv are the panel voltage and current, respectively, Ppv is the panel output power, Vg is the rms value of the grid voltage, sinθ is the in-phase unit vector for the grid voltage, and i∗ is the reference to the current control loop from an MPPT block. As the power reference keeps on changing due to fast MPPT action, the current reference may have a nonzero average value, which is illustrated in Fig. 3 for a step change in power reference which repeats. Assume that a certain amount of dc exists in the current control loop. This will result in applying a voltage with a dc
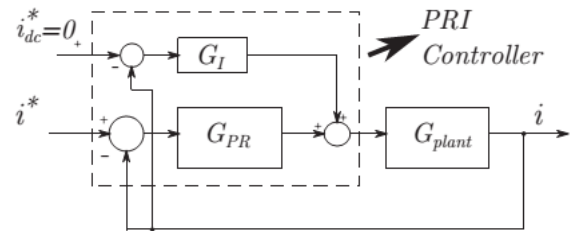
Fig.8. Block diagram of the fundamental current control with the PRI controller.

offset across the L-filter and the transformer primary. The net average current flowing in the filter and the transformer primary loop will be determined by the net resistance present in the loop. This average current will cause a dc shift in the B–H curve of the transformer. This shift would mean an asymmetric nonlinear

saturation characteristic which causes the transformer magnetizing current to lose its half-wave symmetry. The result of this is occurrence of even harmonics. The dc in the system can be eliminated by using the PRI controller.

C) Introduction to the PRI Controller

Conventional stationary reference frame control consists of a PR controller to generate the inverter voltage reference. In this project, a modification to the PR controller is proposed, by adding an integral block, GI as indicated in Fig. 4. The modified control structure is termed as a PRI controller.

$$G_I = \frac{K_I}{s}$$

$$G_{PR}(s) = K_p + \frac{K_r s}{s^2 + \omega_o^2} \qquad \ldots\ldots\ldots 4$$

The plant transfer function is modeled as

$$G_{plant}(s) = \frac{V_{dc}}{R_s + sL_s} \qquad \ldots\ldots\ldots 5$$

This is because the inverter will have a gain of Vdc to the voltage reference generated by the controller and the impedance offered is given by (Rs+sLs) in s-domain. Rs and Ls are the net resistance and inductance referred to the primary side of the transformer, respectively. Ls includes the filter inductance and the leakage inductance of the transformer. Rs is the net series resistance due to the filter inductor and the transformer. The PRI controller is proposed to ensure that the output current of the system does not contain any dc offset. The PRI controller introduces a zero at s=0in the closed-loop transfer function. Hence, the output current will not contain any steady state dc offset. This is necessary in the topology considered because the presence of a dc offset would result in a flow of even harmonics. The following section explains the design of PR controller parameters and proposes a systematic method of selecting and tuning the gain of the integral block in the PRI controller.

III. ADAPTIVE HARMONIC COMPENSATION

A) Review of the LMS Adaptive Filter

The adaptive harmonic compensation technique is based on the usage of an LMS adaptive filter to estimate a particular harmonic in the output current. This is then used to generate a counter voltage reference using a proportional controller to attenuate that particular harmonic. Adaptive filters are commonly used in signal processing applications to remove a particular sinusoidal interference signal of known frequency. Fig. 3.10 shows a general adaptive filter with N weights. The weights are adapted by making use of the LMS algorithm.
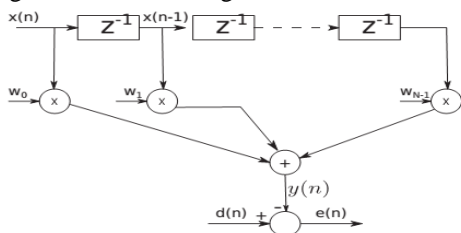
Fig. 9. Structure of a generalized adaptive filter with adaptation weights w_i

For Fig. 9, coefficient vector is defined as

$$\overline{w} = \begin{bmatrix} w_o & w_1 & \ldots & w_{N-1} \end{bmatrix}^T \qquad \ldots\ldots\ldots\ldots 6$$

Input vector and filter output are given in

$$\overline{x}(n) = \begin{bmatrix} x(n) & x(n-1) & \ldots & x(n-N+1) \end{bmatrix}^T$$

$$y(n) = \overline{w}^T \overline{x}(n). \qquad \ldots\ldots 7$$

The error signal is

$$e(n) = d(n) - y(n) \qquad \ldots 8$$

Here, d(n) is the primary input. A frequency component of d(n) is adaptively estimated by y(n). Now, a performance function is defined for the LMS adaptive filter as

$$\zeta = e^2(n) \qquad \ldots 9$$

In any adaptive filter, the weight vector w is updated such that the performance function moves toward its minimum. Thus

$$\overline{w}(n+1) = \overline{w}(n) - \mu \nabla (e(n)^2) \qquad \ldots 10$$

In (3.25), μ is the step size. The convergence of the adaptive filter depends on the step size μ. A smaller value would make the adaptation process very slow whereas a large value can make the system oscillatory. ∇is defined as the gradient of the performance function with respect to the weights of the filter. The final update equation for weights of an LMS adaptive filter can be shown to be

$$\overline{w}(n+1) = \overline{w}(n) + 2\mu e(n)\overline{x}(n) \qquad \ldots 11$$

Thus, from a set of known input vector x(n), a signal y(n) is obtained by the linear combination of x(n)and the weight vector w(n)as in (3.22). Signal y(n)is an estimate of the signal d(n)and the weight vector is continuously updated from (3.28) such that the LMS error e(n)=d(n)−y(n)is minimized. This concept can be used to estimate any desired frequency component in a signal d(n). The adaptive filter used for this purpose will take the reference input x(n)as the sine and cosine terms at that desired frequency. The weight vector will contain two components which scale the sine and cosine and add them up to get an estimated signal y(n). The weights will then be adapted in such a way as to minimize the LMS error between d(n) and y(n). In steady state, estimated signal y(n)will equal the frequency component of interest in d(n).

B) Adaptive Harmonic Compensation

The LMS adaptive filter discussed previously can be used for selective harmonic compensation of any quantity, say grid current. To reduce a particular lower order harmonic (say ik)of grid current:

1) ik is estimated from the samples of grid current and phase locked loop (PLL) unit vectors at that frequency;
2) a voltage reference is generated from the estimated value of ik;
3) Generated voltage reference is subtracted from the main controller voltage reference.

Fig. 3.11 shows the block diagram of the adaptive filter that estimates the kth harmonic ik of the grid current i. The adaptive block takes in two inputs sin(kω_ot) and cos(kω_ot)from a PLL. These samples are multiplied by the weights Wcos and Wsin.

The output is subtracted from the sensed grid current sample, which is taken as the error for the LMS algorithm. The weights are then updated as per the LMS algorithm and the output of this filter would be an estimate of the kth harmonic of grid current. The weights update would be done by using the equations given next, where Ts is the sampling time, e(n)is the error of nth sample, and μ is the step size

$$e(n) = i(n) - i_k(n)$$

.....12
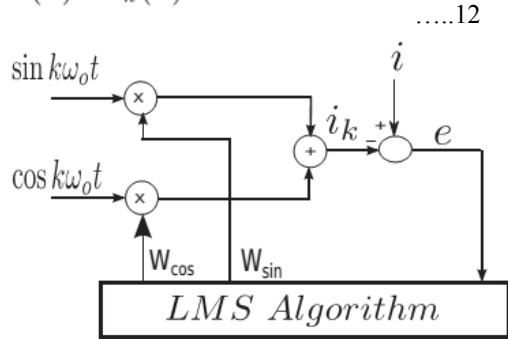
Fig. 10. Block diagram of adaptive estimation of a particular harmonic of grid current.
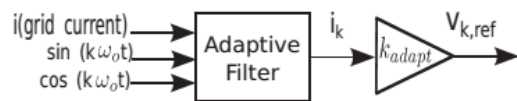
Fig. 11. Generation of voltage reference from estimated kth harmonic component of current using the LMS adaptive filter.

$$W_{\cos}(n+1) = W_{\cos}(n) + 2\mu e(n)\cos(k\omega_o nT_s)$$

$$W_{\sin}(n+1) = W_{\sin}(n) + 2\mu e(n)\sin(k\omega_o nT_s).$$

...13

Now, a voltage reference has to be generated from this estimated current. In this paper, the proportional gain method is used as it is very simple for both design and implementation and is verified to meet harmonic requirements. Fig. 3.12 shows the scheme used for harmonic voltage reference generation from estimated harmonic current. The overall current control block diagram with the adaptive compensation is shown in Fig. 3.13. Note that the fundamental current control is done using the transformer primary current and the harmonic compensation block uses the secondary current, which is the current injected into the grid.

Fig. 3.10 shows only one adaptive harmonic compensation block for the kth harmonic. If say dominant harmonics third, fifth, and seventh need to be attenuated, then three adaptive filters and three gain terms kadapt are required and the net voltage reference added to the output of the PRI controller will be the sum of the voltage references generated by each of the block. Thus, depending on the number of harmonics to be attenuated, the number of blocks can be selected. Note that nin Fig. 11 is the transformer turns ratio from secondary to primary. isec, k,t is the net kth harmonic current in the secondary, which is estimated using the LMS adaptive filter. This is mainly due to the harmonics in the magnetizing current and the dead-time effect. A single-phase PLL is used to generate the reference sine–cosine signals synchronized with the grid voltage for the adaptive filter.
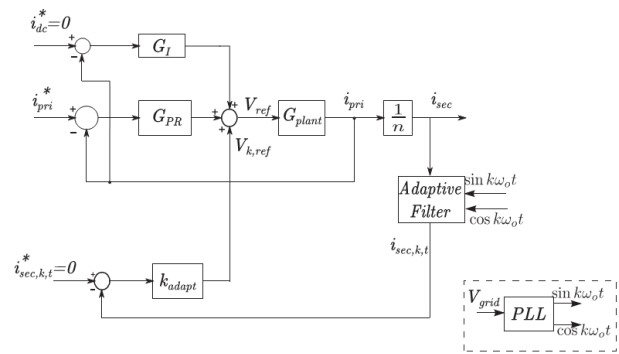
Fig. 12. Complete ac current control structure of the inverter.

IV.   SIMULATION RESULTS

The proposed grid connected single phase and three phase photovoltaic system is simulated in mat lab/Simulink platform. The fig 13 shows the simulated circuit proposed converter without adaptive filter. Fig 16. Shows simulation of single phase circuit with adaptive filter. The simulation study gave results of proposed system with and without adaptive filter for harmonic elimination. The 3rd , 5th , 7th and 9th harmonics are being eliminated from the system with the help of Least mean square algorithm with appropriate weights. The same concept is also applied to three phase system for the harmonic elimination.
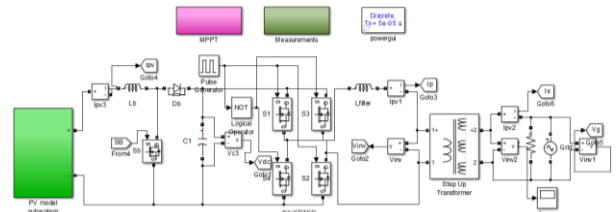
Fig 13. Simulation diagram of the proposed circuit without Adaptive Filter.
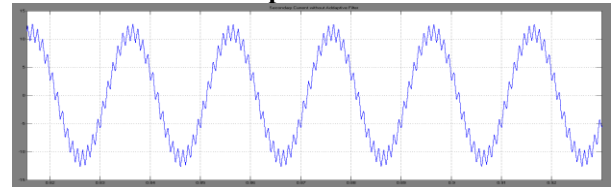
Fig 14. Transformer Secondary Current (Load side) without Adaptive filter
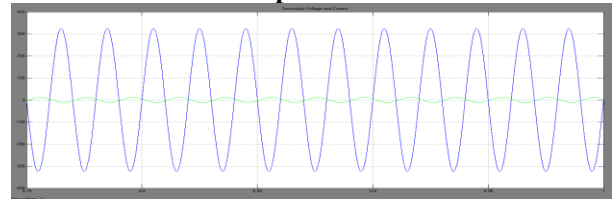
Fig 15. Transformer Secondary Voltage and Current without Adaptive filter

The proposed circuit is simulated in MATLAB/Simulink platform. The simulation results of proposed circuit without adaptive filter had shown the distortion in the transformer currents and voltages and the THD of 11.83% in primary current, 11.80% in secondary current.

Fig 16. Simulation diagram of the proposed circuit with Adaptive Filter.
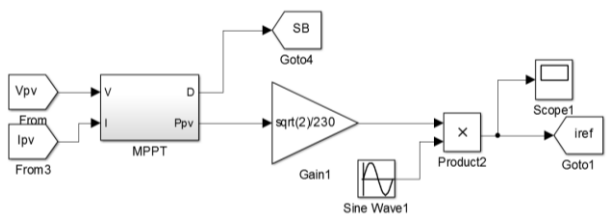
Fig 17. Simulation diagram showing MPPT Controller and Reference Current Generation.
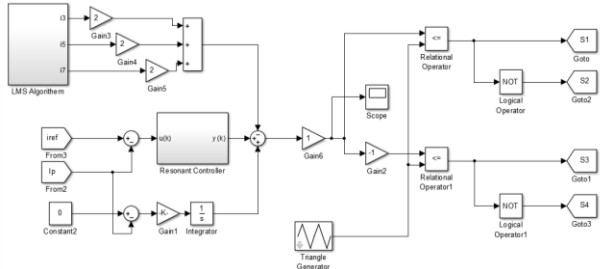
Fig 18. Simulation diagram showing Adaptive filter and Pulse Generation.
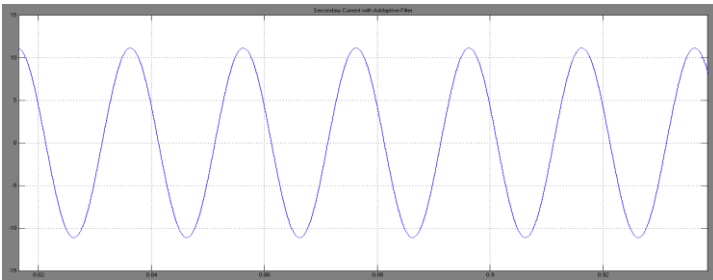
Fig 19. Transformer secondary Current (Load side) with Adaptive filter
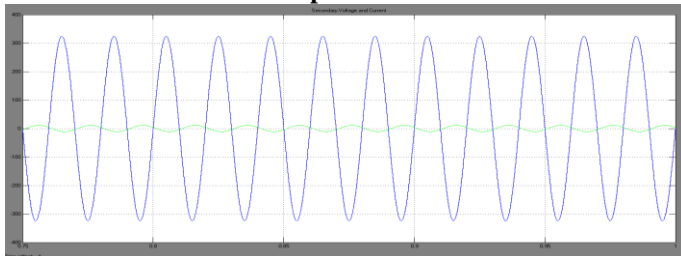
Fig 20. Transformer Secondary Voltage and Current with Adaptive filter

When the proposed circuit is simulated by implementing Adaptive filter the distortion in voltages and currents of transformer are reduced and THD also reduced i.e lower order harmonics are eliminated with the help of Adaptive filter. The

THDs of transformer currents and voltages under both operating conditions are given below.

Table 1. THDs of Transformer Currents

Name	THD Without Filter	THD With Filter
Primary Current	11.83%	0.23%
Secondary Current	11.80%	0.23%

Fig 21. Simulation diagram of the proposed circuit in three phase mode with Adaptive Filter
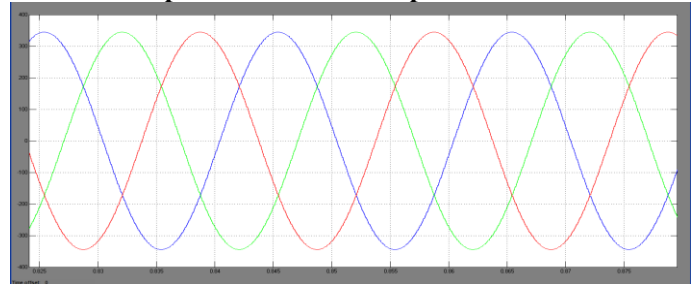
Fig 22. Three Phase Transformer Secondary Voltages.
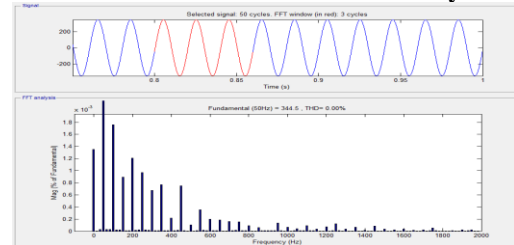
Fig 23. THD of Secondary Current.

V. CONCLUSION

Modification to the inverter current control for a grid connected three-phase photovoltaic inverter has been proposed in this paper, for ensuring high quality of the current injected into the grid. For the power circuit topology considered, the dominant causes for lower order harmonic injection are identified as the distorted transformer magnetizing current and the dead time of the inverter. A novel solution is proposed to attenuate all the dominant lower order harmonics in the system. The proposed method uses an LMS adaptive filter to estimate a particular harmonic in the grid current that needs to be attenuated. The estimated current is converted into an equivalent voltage reference using a proportional controller and added to the inverter voltage reference. The design of the gain of a proportional controller to have an adequate harmonic compensation has been explained. The complete current control scheme consisting of the adaptive harmonic compensation and the PRI controller has been verified experimentally and the

results show good improvement in the grid current THD once the proposed current control is applied.

REFERENCES

[1] Y. Li, S. Jiang, J. G. Cintron-Rivera, and F. Z. Peng, "Modeling and control of quasi-z-source inverter for distributed generation applications," IEEE Trans. Ind. Electron., vol. 60, no. 4, pp. 1532–1541, Apr. 2013.

[2] Y. Huang, M. Shen, F. Z. Peng, and J. Wang, "Z -Source inverter for residential photovoltaic systems," IEEE Trans. Power Electron., vol. 21, no. 6, pp. 1776–1782, Nov. 2006.

[3] D. Cao, S. Jiang, X. Yu, and F. Z. Peng, "Low-cost semi-Z-source inverter for single-phase photovoltaic systems," IEEE Trans. Power Electron., vol. 26, no. 12, pp. 3514–3523, Dec. 2011.

[4] W. Wei, H. Liu, J. Zhang and D. Xu, "Analysis of power losses in Z-source PV grid-connected inverter," in Proc. IEEE 8th Int. Conf. Power Electron. ECCE Asia, May 30–Jun. 3, 2011, pp. 2588–2592.

[5] T. W. Chun, H. H. Lee, H. G. Kim, and E. C. Nho, "Power control for a PV generation system using a single-phase grid-connected quasi Z-source inverter," inProc. IEEE 8th Int. Conf. Power Electron. ECCE Asia,May 30–Jun. 3, 2011, pp. 889–893.

[6] L. Liu, H. Li, Y. Zhao, X. He, and Z. J. Shen, "1 MHz cascaded Z-source inverters for scalable grid-interactive photovoltaic (PV) applications using GaN device," inProc. IEEE Energy Convers. Congr. Expo., Sep. 17–22, 2011, pp. 2738–2745.

[7] B. Ge, Q. Lei, F. Z. Peng, D. Song, Y. Liu, and A. R. Haitham, "An effective PV power generation control system using quasi-Z source inverter with battery," in Proc. IEEE Energy Convers. Congr. Expo., Sept. 17–22, 2011, pp. 1044–1050.

[8] Y. Zhou, L. Liu, and H. Li, "A high-performance photovoltaic module integrated converter (MIC) based on cascaded quasi-Z-source inverters (qZSI) using eGaN FETs," IEEE Trans. Power Electron., vol. 28, no. 6, pp. 2727–2738, Jun. 2013.

[9] Y. Zhou and H. Li, "Analysis and suppression of leakage current in cascaded-multilevel-inverter-based PV systems," IEEE Trans. Power Electron., vol. 29, no. 10, pp. 5265–5277, Oct. 2014.

[10] L. Liu, H. Li, Y. Xue and W. Liu, "Decoupled active and reactive power control for large-scale grid-connected photovoltaic systems using cascaded modular multilevel converters,"IEEE Trans. Power Electron., vol. 30, no. 1, pp. 176–187, Jan. 2015.

[11] D. Sun, B. Ge, F. Z. Peng, A. R. Haitham, D. Bi, and Y. Liu, "A new grid-connected PV system based on cascaded H-bridge quasi-Z source inverter," in Proc. IEEE Int. Symp. Ind. Electron., May 28–31, 2012, pp. 951–956.

[12] Y. Liu, B. Ge, A. R. Haitham, and F. Z. Peng, "A modular multilevel space vector modulation for photovoltaic quasi-Z-source cascade multilevel inverter," inProc. IEEE App. Power Electron. Conf., Mar. 17–21, 2013, pp. 714–718.

[13] F. Guo, L. Fu, C. Lin, C. Li, W. Choi and J. Wang, "Development of an 85-kW bidirectional quasi-Z-source inverter with DC-link feed-forward compensation for electric vehicle applications,"IEEE Trans. Power Electron., vol. 28, no. 12, pp. 5477–5488, Dec. 2013.

[14] T. P. Parker (May 2011). "Reliability in PV inverter design: black art or science-based discipline?" Solarbridge Technologies white paper [Online]. Available:http://solarbridge.wpengine.netdnacdn.com/wpcontent/uploads/2011/05/SLB_E_Design_Reliability.pdf

[15] Y. Liu, A. R. Haitham, B. Ge, D. Sun, H. Zhang, D. Bi, and F. Z. Peng, "Comprehensive modeling of single-phase quasi-Z-source photovoltaic inverter to investigate low-frequency voltage and current ripples," in Proc. IEEE Energy Convers. Congr. Expo., Sept. 14–18, 2014, pp. 4226–4231.

[16] D. Sun, B. Ge, X. Yan, D. Bi, A. R. Haitham, and F. Z. Peng, "Impedance design of quasi-Z source network to limit double fundamental frequency voltage and current ripples in single-phase quasi-Z source inverter," in Proc. IEEE Energy Convers. Congr. Expo., Sept. 15–19, 2013, pp. 2745–2750.

[17] Z. Gao, Y. Ji, Y. Sun, and J. Wang, "Suppression of voltage fluctuation on DC link voltage of Z-source,"J. Harbin Univ. Sci. Techol., vol. 16, no. 4, pp. 86–89, 2011.

[18] Y. Yu, Q. Zhang, B. Liang, and S. Cui, "Single-phase Z-Source inverter: analysis and low-frequency harmonics elimination pulse width modulation," in Proc. IEEE Energy Convers. Congr. Expo., Sep. 17–22, 2011, pp. 2260–2267.

[19] X. Liu, H. Li and Z. Wang, "A fuel cell power conditioning system with low-frequency ripple-free input current using a control-oriented power pulsation decoupling strategy,"IEEE Trans. Power Electron., vol. 29, no. 1, pp. 159–169, Jan. 2014.

AUTHORS

First Author – G Chandra Sekhar, he received his B.Tech degree in Electrical and Electronics Engineering from Mandava Institute of Engineering and Technology in 2012. He is currently pursuing M.Tech Power Electronics in Amrita Sai Institute of Science and Technology, Paritala, A.P, India. His interested research areas are Power Electronic Applications to ASDs.

Second Author – P Rama Krishna, he received his B.Tech degree in Electrical and Electronics Engineering from Nalanda Institute of Engineering and Technology, Sattenapalli (A.P), India, in 2012. M.Tech degree in Power Electronics from Mother Theresa Institute of Science and Technology, Sattupalli (Telangana), India, in 2014. He is currently working as a Assistant Professor in Amrita Sai Institute of Science and Technology, Paritala, A.P, India. His interested research areas are Power Electronics & Drives and Power System.